scientific reports

Check for updates

OPEN

Direct crosstalk between adult human retinas as suggested by interocular transfer of neurovascular coupling through photic stimulation

João Jordão[1], João Figueira[2,3], Miguel Morgado[1,4], Pedro Guimarães[1,2], Pedro Serranho[1,5], Daniela Castro-Farías[6], Delia Cabrera DeBuc[7], Miguel Castelo-Branco[1,2], Michel Paques[6] & Rui Bernardes[1,2]✉

Crosstalk mechanisms between retinas were never documented in humans despite being documented for several other species, including non-human primates. Results of the first-in-human study that documents the crosstalk between retinas by measuring the vascular response in one retina to the photic stimulation of the contralateral eye in health and disease are reported herein. A stimulation apparatus was developed and integrated into an adaptive-optics fundus camera to image 32 healthy control (HC) subjects and 20 type 1 diabetes mellitus (DM) patients. Ipsilateral and contralateral neurovascular coupling effects were documented, and criteria were established to consider an actual response and find positive and negative responses. Ten (31.2%) and two (6.2%) subjects of the HC group presented contralateral positive and negative responses, respectively, and three (15.0%) positive and four (20.0%) negative responses were found for the DM group. Also, statistically significant differences in the ipsilateral ($p < 0.001$) and contralateral ($p = 0.027$) responses were found for the HC group, rejecting the null (non-response) hypothesis. This finding raises the need to revisit the current knowledge of neurovascular coupling mechanisms and the association between its dysregulation and neurological disorders. Further studies involving distinct populations and imaging centers are necessary to validate the findings herein.

Keywords Neurovascular coupling, Circulation, Central nervous system, Retina, Functional imaging, Flicker-induced hyperemia

The complexity of the human central nervous system (CNS) is undisputable and broadly recognized. Also, any change in it has a potentially massive impact on people's daily lives. Therefore, specific knowledge of the CNS function and arrangement is paramount and attracts a substantial research focus. Unveiling new communication channels across its different parts will bring additional insight into this fundamental system.

Neurovascular coupling (NVC)[1] is a well-established effect in which the CNS reacts to stimuli by increasing the local blood flow to satisfy the elevated demand for oxygen due to the increased activity, a fundamental task as the CNS lacks a fuel reservoir to suppress energy needs[2]. Roy and Sherrington[3] initially noted this effect, which has been further demonstrated in the brain and the retina across species[4,5]. Despite its fundamental role and the fact that its impairment has been associated with a variety of disorders, including glaucoma, macular

[1]University of Coimbra, Institute for Nuclear Sciences Applied to Health (ICNAS), Coimbra Institute for Biomedical Imaging and Translational Research (CIBIT), Coimbra, Portugal. [2]University of Coimbra, Faculty of Medicine, Clinical and Academic Centre of Coimbra (CACC), Coimbra, Portugal. [3]University of Coimbra, Faculty of Medicine, Department of Ophthalmology, Coimbra Hospital and University Centre (CHUC), Coimbra, Portugal. [4]University of Coimbra, Faculty of Science and Technology, Department of Physics, Coimbra, Portugal. [5]Department of Sciences and Technology, Universidade Aberta, Lisboa, Portugal. [6]Centre Hospitalier National des Quinze-Vingts, Paris Eye Imaging, Paris, France. [7]Bascom Palmer Eye Institute, University Miami Miller School of Medicine, Miami, FL, USA. ✉email: rmbernardes@fmed.uc.pt

degeneration, Alzheimer's disease, cognitive dysfunction, and diabetes[2], the complete NVC mechanism is still not fully understood.

In this work, we aim to demonstrate the existence of a functional crosstalk mechanism between human retinas in the adult and in vivo.

Demonstrating a vascular response in the retina to stimuli of the contralateral eye and the distinct responses in health and disease support the crosstalk mechanism and add to current knowledge on the NVC mechanism. Moreover, it paves the way for further discoveries and the use of NVC to detect, assess, and monitor vascular-associated diseases.

However, the distant modulation of the vascular network, particularly concerning the communication between retinas, implies a long communication channel yet to be documented.

While the extensive innervation of the vascular network[6] did not raise any questions on the NVC existence in the brain, mechanisms of autoregulation control in the retina are still poorly understood[7–10]. Also, the support for local neural control came from the comparison with the brain[11].

The demonstration of the NVC coupling did not come without discussion. In[12], the authors stated that all techniques measure distinct parts of the complex nature of the blood flow and, therefore, reaction to metabolic demands depends on the region observed. Moreover, the numerous mechanisms involved in vessel diameter regulation represent a complex closed-loop biological control system.

The limits of innervation of the vascular network in the eye[8] are still based on the works of Ehinger and Laties[13,14]. The innervation of the central retinal artery (CRA) is dense along its course within the optic disc, but vessels in the retina "almost completely lack extrinsic innervation"[15]. On the other hand, the concept of intrinsic innervation has been proposed repeatedly[16].

Whether arterioles are the primary site of blood flow regulation remains to be determined in the brain. During neurovascular coupling, the local dilation of arterioles in an activation area will not substantially increase blood flow unless upstream vessels also dilate. How vasodilator and vasoconstrictor responses are conveyed to upstream locations is unclear[17]. The same question can be raised for the retina, and the answer may rely on coupling and communication between cells within the vessel wall. Indeed, through gap junctions between adjacent vascular smooth muscle cells, the brain's intramural propagation of vascular signals produces remote vasodilatation of upstream pial arterioles[18,19].

The retinal crosstalk in the mammalian visual system is demonstrated in[20]. In this work, the authors illustrate the presence of direct communication between the eyes of adult mammals (rats) able to change retinal activity and leave the door open for this effect in other species.

While anatomical evidence for cortico-retinal and retino-retinal projections is substantial[20], there is a lack of physiological evidence for the human species.

The standard view of the adult visual system stipulates that the axons of retinal ganglion cells (RGC) exit the eye to form the optic nerve, with nasal fibers projecting along the contralateral optic tract and temporal fibers along the ipsilateral optic tract to the lateral geniculate nucleus (LGN) and other brain areas. Nevertheless, a diversity of connections exists during embryogenesis and early development but are pruned to form the mature pathway[21–23].

Anatomical studies that have started with the work of Santiago Ramón y Cajal have shown that the optic nerves of adult mammals, including humans[24,25], contain sparse populations of efferent fibers. These originate from multiple locations, including the brain stem and hypothalamus[26–29] and the contralateral eye in young mice[30]. As a matter of fact, "the existence of neurons extending from one retina to the other has been reported during the perinatal development in different vertebrates"[30]. Although initially believed to be artifacts or misprojections, their presence was unequivocally demonstrated for a small subset of RGC in mice[30].

The efferent fibers branch in the eye covers approximately a quarter of the retinal surface[28]. Their branches terminate in the inner and outer plexiform layers (IPL, OPL), inner nuclear layer (INL), and ganglion cell layer (GCL) depending on fiber type[25,31–33]. Hence, even few, there may be retinal efferent fibers in adult mammals with potential impact on several mechanisms, control, and function.

While the efferent innervation of the retina has now been widely documented in rodents and other animals, e.g., birds, rabbits, and cats[20,34–38], the existence and function of an efferent system in humans and non-human primates remains to be definitively established. Yet, their presence (efferent innervation, not retina-retina fibers) is strongly suggested based on non-tracing and tracer methods/immunohistochemistry for Chimpanzees, Macaca mulatta, Saimiri sciureus, Macaca fascicularis, Macaca nemestrina, Papio anubis, and Cebuspaella[39].

Concerning humans, all anatomical evidence was generated from autopsy cases or eyes removed during surgery. Morphological studies of an enucleated eye, ten days after complete occlusion of the CRA, showed that all ganglion cells and afferent neurites had degenerated. In contrast, all of the presumed efferent nerves with their cell bodies in the brain were still present in the optic disc[39].

In the present study, an adaptive-optics (AO) fundus camera (rtx1) from Imagine Eyes (Imagine Eyes, Orsay, France) was used to scan the retinas of a group of healthy controls and a group of type 1 diabetes mellitus patients. The camera was equipped with an in-house built apparatus to stimulate the non-imaged eye synchronously with the acquisition of fundus images to document the contralateral response. The gathered data show the vascular response in the imaged eye to the stimulus of the contralateral eye and a distinct response pattern of the diabetic group from that of the healthy group, therefore supporting the presence of a functional crosstalk mechanism between retinas never documented in the human species.

Methods

Neurovascular coupling is the alteration in local perfusion in response to changes in energy demands due to neuronal activity. To quantify it, the variation in vessel lumen at the same vessel section, before and after

stimulation, is measured and then expressed as a percentage (% var). This method disregards differences in vessel calibers, facilitating comparisons across various subjects.

Instrumentation

An rtx1 adaptive-optics fundus camera from Imagine Eyes was used to gather data in this work. The camera system utilizes an *en-face* reflectance imaging method. It captures images in the near-infrared spectrum (850 nm) using a charge-coupled device (CCD) sensor with low noise and an exposure time of less than 10 ms. It allows for the acquisition of 4 × 4 degree field-of-view (FOV) images of the ocular fundus (1.2 × 1.2 mm^2 FOV, 1500 × 1500 pixels image) with high resolution (2 microns, 250-line pairs per millimeter)[40,41]. The rtx1 acquires images with or without stimulating the imaged retina. It allows for different acquisition timings: temporarily overlapping the stimulation, after the end of stimulation, or with a defined delay after stimulation.

The adaptive-optics control is fully automatic and corrects for blinking and saccades. The camera can compensate for refractive errors ranging from −12 D to +6 D, making it suitable for most individuals. Additionally, as an add-on for this study, the rtx1 outputs two 3.3 V digital trigger signals, one enabled during fundus acquisition and the other triggering the flicker stimulation. The rtx1 light flicker stimulus is based on an internal OLED micro-display panel configured to deliver yellow light with a peak wavelength of 570 nm. Henceforth, the flicker of the rtx1 system will be referred to as the "*internal flicker.*"

To establish the presence of a crosstalk mechanism, the NVC effect was assessed in the imaged eye in response to the stimulation of the contralateral one. Custom in-house developed hardware composed of a light source and control system was fully integrated into the rtx1. It synchronizes with the acquisition through the rtx1-trigger signals mentioned above. The apparatus and its parts can be seen in Fig. 1.

The prototype developed for stimulating the non-imaged retina will be referred to as the "*external flicker.*" This prototype consists of two modules, one for inputting trigger signals and the other for controlling the light flickers (Fig. 1). For details, see[42]. The external stimulation was set up with two arrays of seven individually addressable red, green, and blue light-emitting diodes (RGB LED), one for each eye, to allow studying the contralateral effect in the left or right eyes.

The irradiance of the external device was measured using a calibrated SR900 spectrometer (Opsytec Dr. Gröbel, Ettlingen, Germany) to ensure it meets the International Commission on Non-Ionizing Radiation Protection (ICNIRP) guidelines concerning eye exposure limits in conditions of ophthalmic examination[43]. Nevertheless, the LEDs' maximum irradiance was limited in firmware to ensure that a possible communication error would not override settings and exceed exposure limits. The RGB LEDs were configured to achieve a perceived dark yellow color matching the rtx1 internal one.

The external device and the rtx1 are controlled using a custom-developed software application written in C++. The control software integrates with the rtx1's software (AOimage 3.4) and allows the user to specify the settings for the rtx1 camera and the external flicker module (the same parameters' values and trigger signals used for both), namely the duration, flickering frequency and intensity parameters of the stimuli.

Study design and participants

All subjects were instructed not to drink coffee on the day of the examination, and all subjects fulfilled the inclusion and exclusion criteria defined as:

– Inclusion criteria:

- aged 18 to 60, inclusive;
- best corrected visual acuity equal to or over 69 letters (20/40 Snellen scale);
- refractive spherical equivalent between −6 and +5 diopters;
- type I Diabetes Mellitus (for the patient group);
- level 10 of the ETDRS-DRSS scale (for the patient group);
- demographic matching with the patient group (for the healthy group).Exclusion criteria:

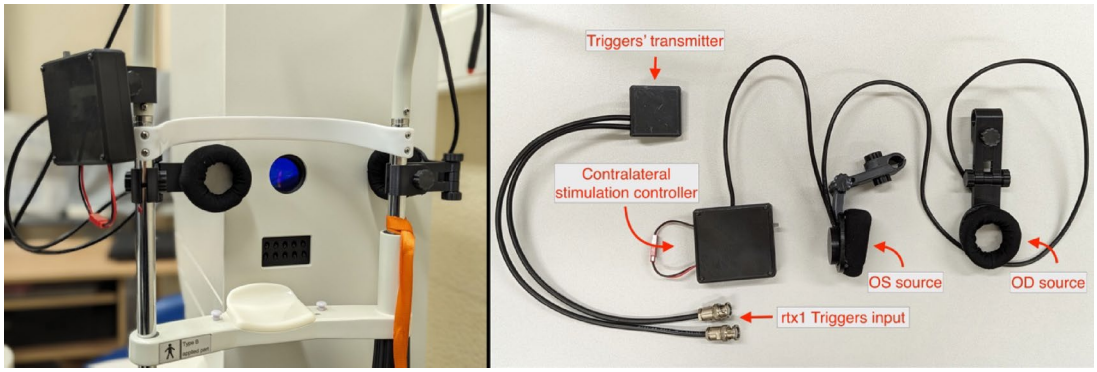

Fig. 1. Left: apparatus installed on the rtx1 (Imagine Eyes). Right: Apparatus parts. The external light sources are fixed to a pair of custom supports covered by foam pads to prevent flicker light from propagating to the imaged retina during contralateral stimulation and provide comfort.

- any ocular diseases that may interfere with the examination of the study eye;
- presence of a history of glaucoma;
- pupillary dilation below 5 mm in the study eye;
- ocular inflammation, conjunctivitis, or any history of uveitis in the study eye;
- signs or history of diabetic macular edema (for the patient group);
- signs or history of retinal vascular disease or neurodegenerative disease, including hypertensive retinopathy in the study eye;
- only one functional eye;
- any previous intravitreous treatment;
- any previous laser treatment in the retina;
- any ocular surgery in the past 6 months before enrollment in the study;
- any signs of arterial obstructive disease;
- any history of thromboembolic events;
- history of central nervous system disorders, neurodevelopment disorders, psychiatric disorders, or auditory or visual deficits;
- pregnant or breastfeeding women;
- history of alcohol or drug abuse.

The dataset used in this cross-sectional study was collected between October 2023 and July 2024 and consists of 32 healthy control subjects (19 females and 13 males, 17 left/15 right eyes, age range: 19–55 years, median 28.5 years, m(sd): 32.7(10.5) years), and 20 type 1 diabetic patients with no signs of diabetic retinopathy (10 females and 10 males, 10 left/10 right eyes, age range: 20–57 years, median 32.0 years, m(sd): 35.0(12.3) years, HbA_{1C} range: 5.8–7.9%, median 6.8%, m(sd): 6.9(0.5)%). All subjects presented a best-corrected visual acuity (BCVA) of 0.00 (logMAR), an intraocular pressure (IOP) of the imaged eye ranging from 10 to 23 mmHg (m(sd): 15.8(3.6) mmHg) and an IOP of the contralateral eye ranging from 10 to 23 mmHg (m(sd): 15.8(3.6) mmHg). Healthy control subjects presented spherical equivalent refractive errors ranging from −4.75 to 2.50 diopters (D) (m(sd): −0.75(1.77) D) for the image eye and −4.75 to 4.38 D (m(sd): −0.82(1.82) D) for the contralateral eye. Diabetic patients presented spherical equivalent refractive errors ranging from −6.00 to 1.25 D (m(sd): −0.89(1.54) D) for the image eye and −6.00 to 1.25 D (m(sd): −0.96(1.64) D) for the contralateral eye. Blood pressure (BP) ranged from 90 to 139 mmHg (m(sd): 116.0(11.3) mmHg) and from 59 to 93 mmHg (m(sd): 73.0(8.1) mmHg), respectively for the systolic and diastolic BP, and was measured for all but the initial 12 healthy controls (HC01 to HC12).

All participants provided written informed consent for the study, which was conducted in accordance with the Declaration of Helsinki and its subsequent revisions. Additionally, ethical approval (CE-039/2023) was obtained from the ethics committee of the Faculty of Medicine of the University of Coimbra.

All patients are regularly followed at the ophthalmology department following the standard protocol for type I diabetic patients and underwent a complete ophthalmic examination at the ophthalmology department of the Coimbra University Hospital before enrollment in the study, which included a slit lamp exam, widefield fundus photography, OCT (Optical Coherence Tomography)(macular and optic disc protocols), OCT-A (OCT – Angiography), and best corrected visual acuity. Besides these data, all patients were checked for the inclusion and exclusion criteria and collection of demographics and anthropometric data, heart blood pressure and metabolic status, hormonal status, relevant family history, medication, and life habits prior to the enrollment in the study.

Only one eye per subject was considered (imaged), selected per group alternatively between the right and left eye at the study enrollment. The experimental procedure begins with measuring the intraocular pressure and applying tropicamide-based mydriatic eye drops to promote mydriasis and cycloplegia.

Two acquisition modes were used: the baseline mode, in which image acquisitions were performed without being preceded by any stimulation, and the stimulation mode, in which image acquisitions immediately follow a stimulation of 20 s of flicker light at 15 Hz (square wave shape and maximum contrast – same contrast for the internal and external stimulators). For both modes, image acquisition lasted 2 s.

After the full dilation, following the application of mydriatic eye drops and keeping subjects in the imaging room in dark conditions, the selected subject's eye was imaged three times without stimulation (*Basal 1*) and immediately imaged three times following the contralateral stimulation (*Contra*) using the external stimulator. A waiting time of 5 min before the next sequence was set to allow the neurovascular coupling to return to a stable state. After that, three acquisitions were performed without any stimulation (*Basal 2*) immediately followed by three acquisitions following the ipsilateral stimulation (*Ipsi*) using the rtx1 internal flicker (Fig. 2). All acquisitions were performed at an artery as close as possible to the subject's fovea, and all acquisitions of the same subject were performed at the same location where the selected artery presents a well-defined lumen and walls. The imaging room was kept in dark conditions for the entire duration of the subject's study.

Data analysis

All acquired images were exported for further processing. A grader manually segmented a vessel portion using custom-made software allowing to zoom in and out, image panning, and mouse pointing at rtx1 images to define the vessel lumen. All 12 images (three images per acquisition type: Basal 1, Contra, Basal 2, and Ipsi) were individually segmented by the same grader. Image examples and respective segmentation can be seen in Fig. 3. One independent grader assessed all segmentations, and another assessed segmentation by sampling the dataset.

A binary mask was defined based on the lumen segmentation, and the vessel centerline was determined from the mask. The same vessel segment limits were used across all images per eye. Per image, the lumen width was defined as the ratio of the area to the length of the segment (length of the centerline), obtaining an estimate of

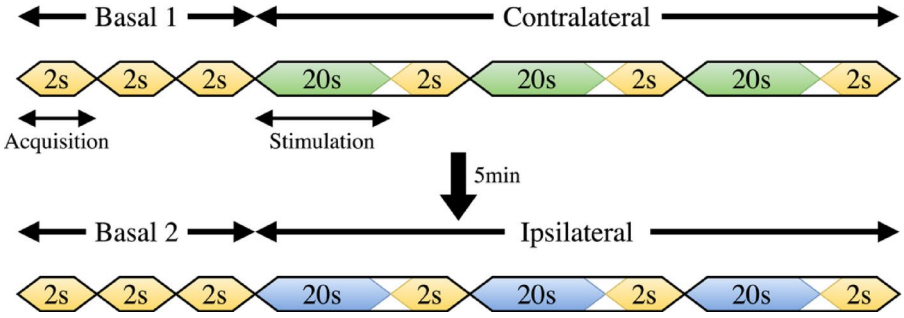

Fig. 2. Sequence and time duration (not-to-scale) of eye fundus acquisition protocol. Each acquisition takes 2 s, preceded or not by a photic stimulation of 20 s. A five-minute interval takes place between the top and bottom sequences.

its average in pixels. The lumen width for each acquisition type was defined as the maximum of the respective three consecutive scans. Each subject has, therefore, four measures of the vessel lumen at the same location. The respective NVC response is defined as the percentage of the relative variation between the lumen values for the baseline and the ones following the stimulation, therefore allowing the comparison of the responses for the different subjects/eyes. The contralateral and the ipsilateral responses were computed as $\%var_{contra} = 100\times(lw_{contra} - lw_{basal1})/lw_{basal1}$ and $\%var_{ipsi} = 100\times(lw_{ipsi} - lw_{basal2})/lw_{basal2}$, respectively, where lw stands for lumen width.

A non-parametric Wilcoxon test for pairwise samples was performed to test whether significant contralateral and ipsilateral responses were found in the healthy group. Also, for both groups, a set of criteria was established to define an individual relevant contralateral response:

C1: only cases where the lumen's width following a contralateral stimulation was either both over basal1 and basal2 lumens (positive response) or under basal1 and basal2 lumens (negative response);

C2: the minimum variation to any of the basal1 or basal2 should be over 10% of the maximum variation to any of these;

C3: the contralateral response should exceed 50% of the minimum ipsilateral response for the entire group;

C4: the contralateral response should be over 1% or exceed 50% of the respective ipsilateral response.

Results

Raw data can be seen in Table 1; Figs. 4 and 5.

For the healthy control group, a statistically significant difference was found between the contralateral and ipsilateral NVC and the previous basal state, respectively, $p = 0.027$ and $p < 0.001$ (Wilcoxon test), rejecting the null hypothesis of no response in both cases.

Of the 32 healthy controls, 24 (75.0%) presented a contralateral positive response (please note the marginal positive response of the HC09 subject). Twenty subjects (62.5%) verified criteria C1 to C3 (Fig. 6). Twelve healthy controls (37.5%) verified criteria C1 to C4, ten subjects (83.3%) presented positive contralateral responses, and two individuals (16.7%) presented negative contralateral responses (Fig. 7).

For the diabetic group, 13 individuals (65.0%) presented a negative contralateral response (Fig. 5). Twelve subjects (60.0%) verified criteria C1 to C3 (Fig. 8). Seven subjects (35.0%) verified criteria C1 to C4, three with a positive and four with a negative contralateral response (Fig. 9).

These results support the NVC reflex in response to the stimulation of the contralateral eye, with 12/32 (37.5%) healthy controls and 7/20 (35.0%) type 1 diabetes mellitus patients fulfilling the established criteria, implying a response followed by a return to the baseline condition.

Discussion

For the first time, we have imaged the human retina with an adaptive-optics fundus camera equipped with an external stimulation apparatus to allow the photic stimulation of the contralateral eye.

The same eye of each subject was imaged first without being stimulated (basal measurement) and after the stimulation of the contralateral eye. After a period of 5 min, the same eye was imaged again, without being stimulated (new basal) and after its ipsilateral stimulation. The same vessel portion was analyzed by segmenting the vessel's lumen. The average lumen width for each of the four scenarios was computed, and the response to the stimulus was determined as the percentage of variation in the lumen width in relation to the respective basal value to account for temporal variations in the basal lumen. We have shown that there is a response to the contralateral stimulation by demonstrating that the computed variation in lumen obeys several criteria (for the healthy and patient groups) and has a statistically significant difference from the null hypothesis (no response) for the healthy control group.

How the information propagates from one eye to the other is still unknown. However, a mechanism similar to the one in the brain, where through gap junctions between adjacent vascular smooth muscle cells the brain's intramural propagation of vascular signals produces remote vasodilatation of upstream pialarterioles[18,19], associated with the dense innervation of the CRA and the local propagation of vasodilatory signals, suggest this as a potential mechanism for the contralateral NVC effect in the retina.

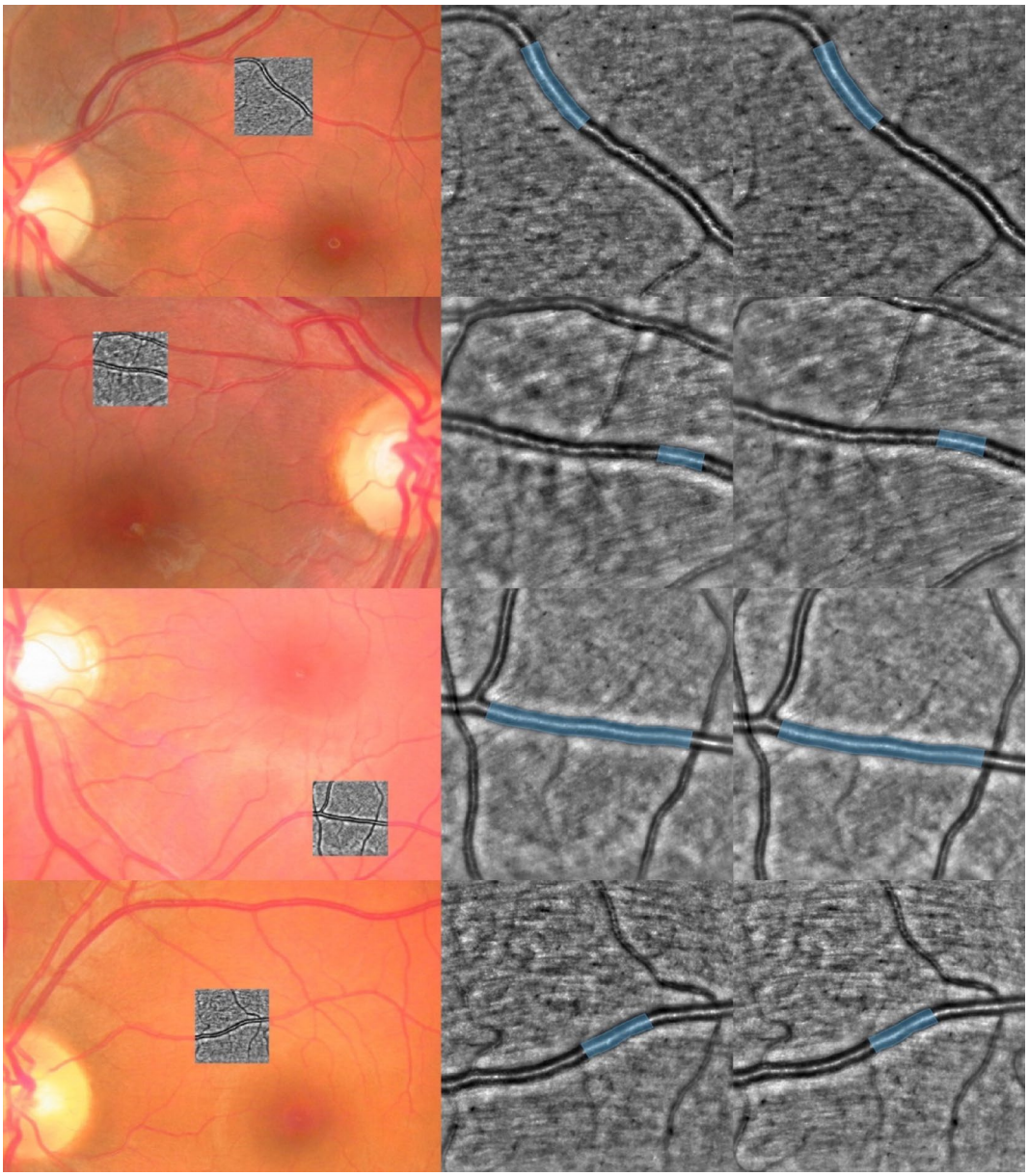

Fig. 3. Two healthy control (top) and two diabetic patients (bottom) examples. From top to bottom: cases HC03, HC08, DM02 and DM04. Left: color fundus photography with the rtx1 shown overlapped in grayscale. Middle/Right: full-size rtx1 images (4 × 4 degree field-of-view, 1500 × 1500 pixels) after the contralateral/ipsilateral stimulation. Analyzed vessel segment in blue. Additional example cases can be seen in the Supplementary figures.

In addition to demonstrating the crosstalk between adult human retinas, we have shown that the mechanism is present both in health and disease (type 1 diabetes). Our results also suggest a different response pattern in the patient group.

The main strengths of this study were the use of detailed ophthalmic imaging and the demonstration of the statistically significant difference for the contralateral stimulation in the adult healthy population, in vivo and non-invasively, through the direct evaluations of the change in the vessels' lumen.

Nevertheless, there are some limitations to our study. First, this cross-sectional study has a limited sample size. Second, the study sample might not adequately represent other populations where different response patterns can exist. Additionally, a different set of operating parameters, e.g., stimulation period, a time gap between the stimulation and acquisition, or the acquisition while still stimulating, different stimulation intensities, may show an increased contralateral response. However, for the sake of demonstration of a working mechanism in the adult human retina, the system configuration used proved to be adequate, and the novel findings shed new light on the NVC mechanism, a significant breakthrough because existing NVC models do not consider the demonstrated effect and may need to be revisited.

ID	Type	Sex	Age (years)	BP (mmHg)	HbA_{1C} (%)	Spherical Equivalent Error (D)	Imaged Eye	IOP [mmHg]		Lumen width (pixels)			
								Imaged Eye	Contralateral Eye	Basal 1	Contra	Basal 2	Ipsi
HC01	HC	F	39	NA	NA	0(0)	OS	15	16	119.8	119.1	119.0	120.1
HC02	HC	F	33	NA	NA	−1.25(−1.50)	OD	11	11	49.4	49.9	50.3	51.0
HC03	HC	F	27	NA	NA	−1.25(−1.25)	OS	21	21	86.9	84.5	86.7	92.9
HC04	HC	M	22	NA	NA	0(0)	OD	20	20	104.4	105.0	106.3	109.3
HC05	HC	M	26	NA	NA	−4.75(−4.75)	OS	22	22	78.7	79.9	77.2	80.2
HC06	HC	F	33	NA	NA	−4.25(−4.50)	OD	15	16	89.0	89.9	89.1	91.5
HC07	HC	F	30	NA	NA	0.25(0.25)	OS	10	13	105.6	108.2	104.9	108.8
HC08	HC	F	24	NA	NA	2.00(−0.75)	OD	15	15	80.9	85.6	84.7	88.1
HC09	HC	F	35	NA	NA	−2.63(−2.50)	OS	15	13	51.8	51.9	52.4	55.1
HC10	HC	F	25	NA	NA	−2.25(−2.25)	OD	19	19	84.0	85.2	84.6	86.0
HC11	HC	F	23	NA	NA	−0.50(−1.13)	OS	18	15	93.8	93.3	90.1	98.8
HC12	HC	M	35	NA	NA	1.50(0.25)	OD	20	20	70.9	73.7	71.7	75.8
HC13	HC	F	19	122/59	NA	−1.38(−0.88)	OS	18	18	75.7	76.4	75.2	78.4
HC14	HC	M	24	123/80	NA	−0.25(−0.75)	OD	16	16	96.6	97.4	95.7	98.3
HC15	HC	F	24	110/80	NA	−0.63(−0.50)	OS	20	20	94.1	95.2	93.6	94.9
HC16	HC	M	24	128/65	NA	0(0)	OD	18	20	96.9	96.0	99.1	99.4
HC17	HC	F	24	116/73	NA	−0.88(−1.38)	OD	23	23	76.0	76.2	76.6	77.9
HC18	HC	M	52	120/88	NA	0(0)	OS	20	20	72.4	73.3	71.4	77.0
HC19	HC	F	24	116/73	NA	−3.38(−2.50)	OD	20	20	75.3	74.2	74.3	78.0
HC20	HC	F	52	103/68	NA	2.50(2.25)	OD	10	10	82.8	83.4	82.8	84.4
HC21	HC	F	54	130/79	NA	0.75(0.88)	OS	14	13	71.9	74.2	75.4	78.2
HC22	HC	M	25	98/63	NA	0.25(0.50)	OD	15	15	53.7	54.2	55.1	56.9
HC23	HC	M	41	121/73	NA	−2.63(−3-63)	OS	10	11	102.8	104.3	95.6	104.5
HC24	HC	M	21	124/80	NA	0(0)	OD	12	12	83.6	83.5	84.6	90.0
HC25	HC	F	44	126/73	NA	−2.50(−1.50)	OS	12	12	63.0	63.6	64.4	64.0
HC26	HC	F	45	102/65	NA	−0.63(−1.00)	OD	11	10	104.0	104.1	103.2	104.0
HC27	HC	F	39	108/68	NA	0(0)	OS	15	15	82.2	82.4	81.2	82.9
HC28	HC	F	24	114/62	NA	1.38(4.38)	OS	13	13	102.5	101.6	102.0	105.7
HC29	HC	M	40	110/73	NA	−4.25(−4.00)	OS	11	11	64.5	65.1	65.1	66.1
HC30	HC	M	55	110/70	NA	−0.13(−0.25)	OS	12	12	82.6	82.9	82.4	83.3
HC31	HC	M	24	120/88	NA	0(0)	OS	12	13	88.8	86.1	85.6	91.8
HC32	HC	M	38	102/63	NA	0.88(0.25)	OD	10	10	89.7	90.2	88.4	89.6
DM01	T1DM	F[M]	45	90/66	6.7	0(0)	OD	17	17	66.3	66.1	66.0	66.1
DM02	T1DM	M	24	120/75	6.4	−2.25(−2.75)	OS	16	16	84.7	87.4	86.3	88.3
DM03	T1DM	M	51	116/76	5.8	−2.25(−2.25)	OD	14	14	120.5	122.6	122.7	122.9
DM04	T1DM	M	42	120/60	5.8	−2.38(−2.50)	OS	16	16	80.1	76.7	79.6	81.6
DM05	T1DM	M	57	118/74	6.6	1.25(1.25)	OD	14	14	78.7	78.4	79.0	81.9
DM06	T1DM	M	57	127/79	7.4	−1.13(−1.38)	OS	16	14	72.0	70.7	70.5	72.5
DM07	T1DM	M	22	122/74	6.7	0(0)	OD	18	18	90.8	90.7	92.0	91.6
DM08	T1DM	F	42	123/93	6.8	0(0)	OS	12	12	72.0	72.3	70.1	76.0
DM09	T1DM	F	28	96/71	6.9	0(0)	OD	15	14	85.7	85.0	83.8	85.7
DM10	T1DM	F	22	112/67	7.4	−0.88(−0.38)	OS	20	20	82.7	82.3	83.3	85.2
DM11	T1DM	F	21	105/86	6.7	0(0)	OD	20	20	111.7	110.7	112.3	112.5
DM12	T1DM	F	47	121/73	7.9	0(0)	OD	19	19	77.7	78.0	78.1	79.6
DM13	T1DM	M	25	117/68	6.8	−6.00(−6.00)	OS	20	20	55.7	56.9	56.1	56.5
DM14	T1DM	M	25	132/63	7.6	0(0)	OD	21	21	82.9	82.4	82.7	82.5
DM15	T1DM	M	27	139/72	6.8	−0.50(−0.63)	OS	16	16	103.4	102.8	103.9	106.7

Continued

ID	Type	Sex	Age (years)	BP (mmHg)	HbA_{1C} (%)	Spherical Equivalent Error (D)	Imaged Eye	IOP [mmHg]		Lumen width (pixels)			
								Imaged Eye	Contralateral Eye	Basal 1	Contra	Basal 2	Ipsi
DM16	T1DM	M	44	136/86	7.6	0(0)	OD	16	15	92.5	92.3	91.3	92.6
DM17	T1DM	F	36	98/76	6.7	−2.50(−3.50)	OS	15	18	60.1	60.4	59.4	61.3
DM18	T1DM	F	42	131/80	6.8	0(0)	OS	14	14	82.9	83.8	83.3	83.8
DM19	T1DM	F	20	113/68	7.3	−1.25(−1.00)	OD	21	20	108.6	107.8	107.2	106.0
DM20	T1DM	F	24	103/69	7.2	0(0)	OS	10	10	101.5	99.2	100.1	101.1

Table 1. Raw data and subject characterization. HC – healthy controls; T1DM – type 1 diabetes mellitus; M/F – male/female; $F^{[M]}$ – Menopause; OD/OS – right/left eye; BP – blood pressure; Spherical equivalent error (diopters) for the imaged (non-imaged) eye; IOP – intraocular pressure; Basal 1/2 – acquisitions without stimulation; Contra/Ipsi – acquisition after contralateral/ipsilateral stimulation; NA – not available.

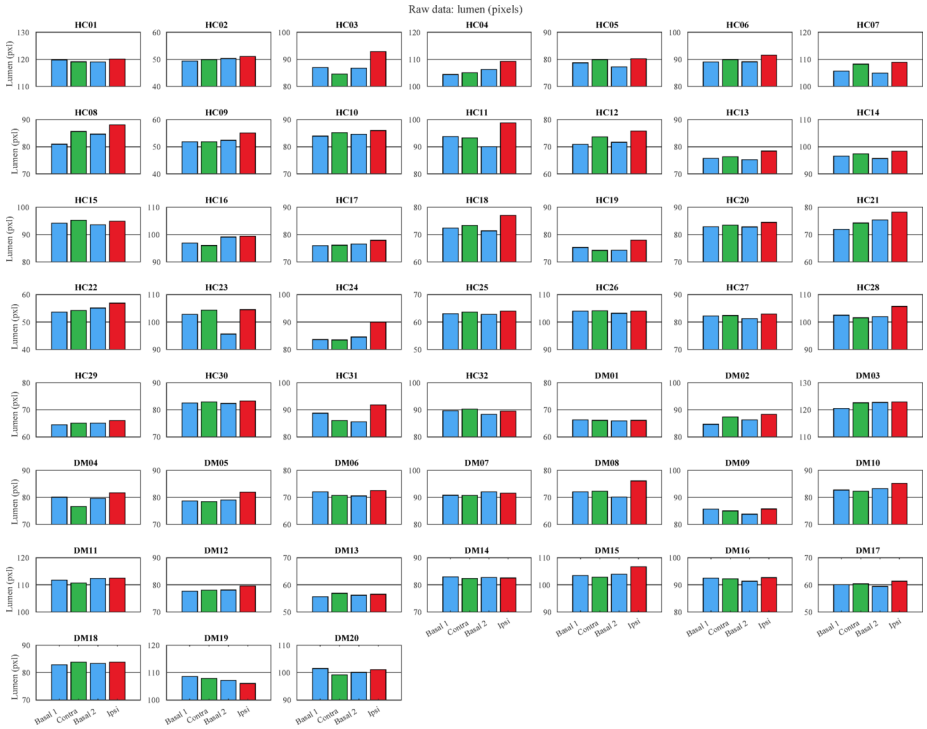

Fig. 4. Lumen width data (in pixels) for all cases in the study (32 healthy controls (HC01-HC32) and 20 type 1 diabetic patients (DM01-DM20)). Color bars, from left to right: "Basal 1" (blue), "Contra" (green - contralateral stimulation), "Basal 2" (blue), and "Ipsi" (red - ipsilateral stimulation).

Demonstrating these effects in a larger population and across different imaging centers is paramount, as well as assessing the pattern of response for several disorders, particularly those known to be associated with vascular changes, including Alzheimer's disease, cognitive dysfunction, and diabetes.

This study's findings are still far from an immediate application in clinical practice, and further studies involving several distinct populations are necessary. However, the prospects for new biomarkers of disease onset, progression, or staging seem to be waiting to be discovered.

Conclusion

We present evidence on the crosstalk between adult human retinas through the modulation of vessels' width in response to the photic stimulation of the contralateral eye. Our results also suggest that this crosstalk mechanism may be modified in type 1 diabetes mellitus patients and may be a biomarker of initial changes not identified by current methods.

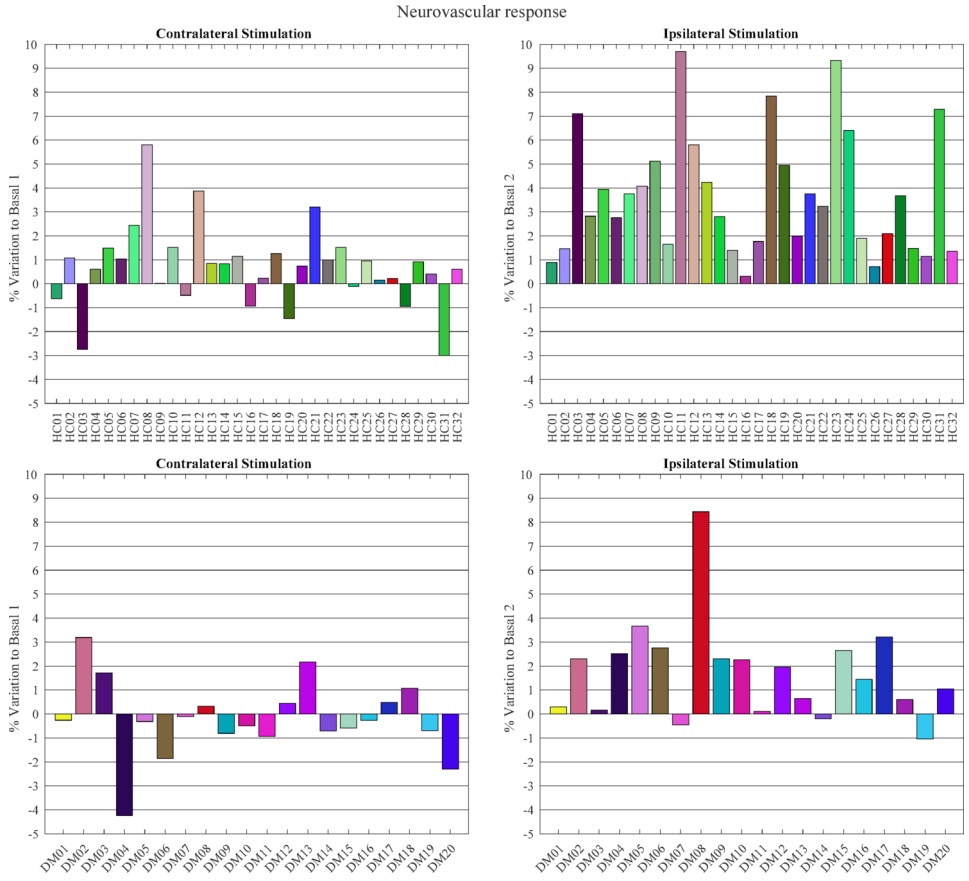

Fig. 5. Neurovascular response data for the health control (top) and the diabetic patient (bottom) groups. Response to the photic stimuli is shown as a percentage of lumen width variation from the basal lumen width. Left: contralateral stimulation response. Right: ipsilateral stimulation response.

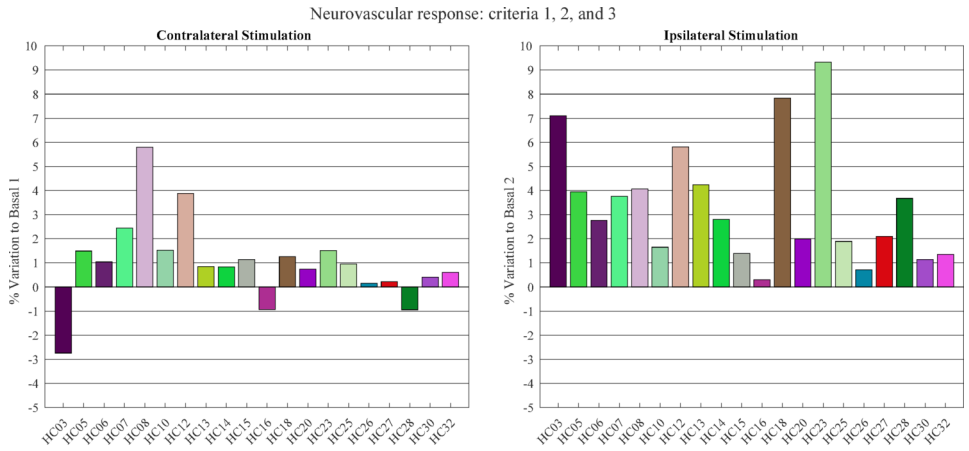

Fig. 6. Healthy control cases (20/32 (62.5%)) for whom the response to the contralateral stimulation recovered totally or partially to the basal lumen value and for whom the response (absolute value) is over half the minimum of the ipsilateral response for the entire set.

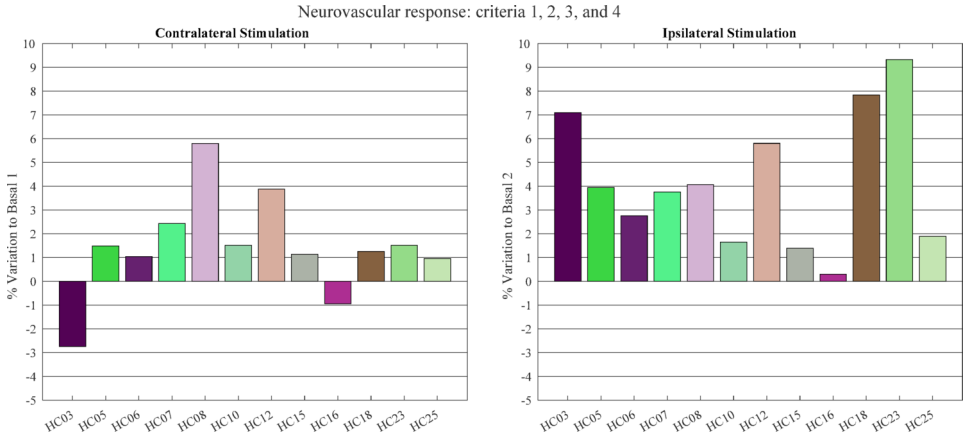

Fig. 7. Healthy control cases (12/32 (37.5%)) for whom the response to the contralateral stimulation recovered totally or partially to the basal lumen value and for which the response (absolute value) is over half the minimum of the ipsilateral response for the entire set, and for whom the contralateral response is over 1% or over half of the ipsilateral response for the same subject.

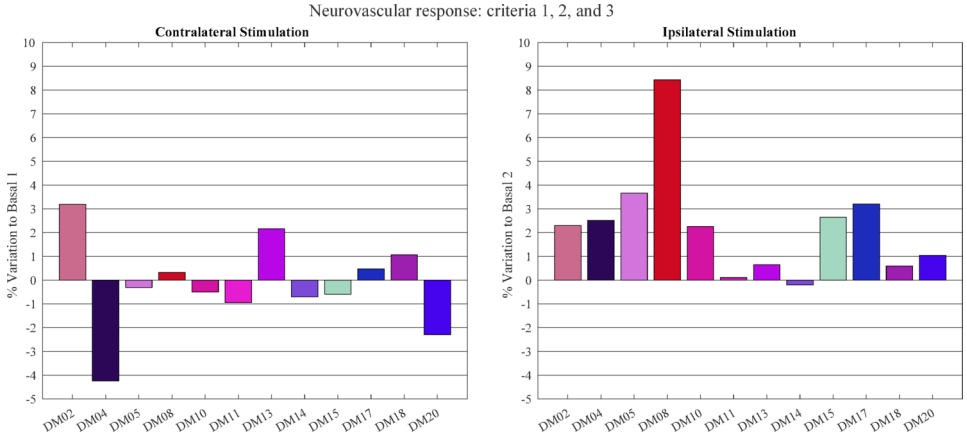

Fig. 8. Type I diabetic patient cases (12/20 (60.0%)) for whom the response to the contralateral stimulation recovered totally or partially to the basal lumen value and for whom the response (absolute value) is over half the minimum of the ipsilateral response for the entire set.

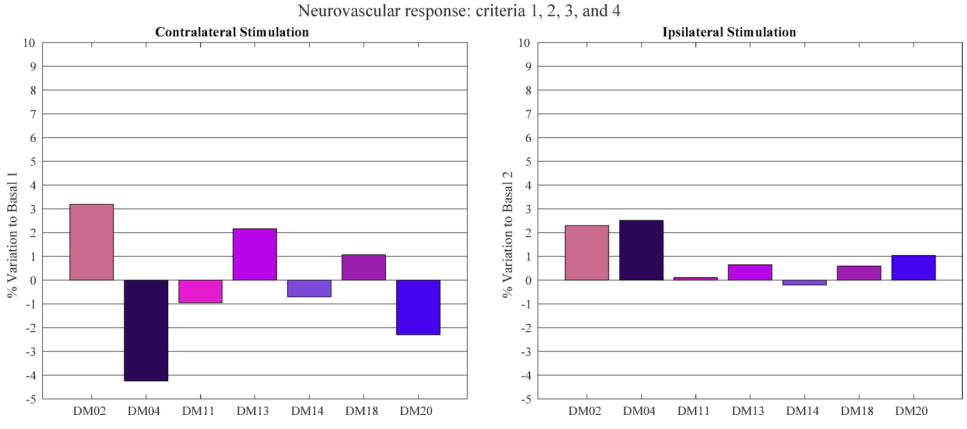

Fig. 9. Type 1 diabetic patient cases (7/20 (35.0%)) for whom the response to the contralateral stimulation recovered totally or partially to the basal lumen value and for which the response (absolute value) is over half the minimum of the ipsilateral response for the entire set, and for whom the contralateral response is over 1% or over half of the ipsilateral response for the same subject.

Data availability

The data supporting the conclusions of this article will be made available by the corresponding author upon formal and reasonable request.

Received: 17 December 2024; Accepted: 14 April 2025
Published online: 21 April 2025

References

1. Attwell, D. et al. Glial and neuronal control of brain blood flow. *Nature* **468** (7321), 232–243. https://doi.org/10.1038/nature09613 (2010).
2. Iadecola, C. The neurovascular unit coming of age: A journey through neurovascular coupling in health and disease. *Neuron* **96** (1), 17–42. https://doi.org/10.1016/j.neuron.2017.07.030 (2017).
3. Roy, C. S. & Sherrington, C. S. On the regulation of the Blood-supply of the brain. *J. Physiol.* **11** (1–2), 85–158. https://doi.org/10.1113/jphysiol.1890.sp000321 (1890).
4. Lecleire-Collet, A. et al. Evaluation of retinal function and flicker light-induced retinal vascular response in normotensive patients with diabetes without retinopathy. *Investig. Ophthalmol. Vis. Sci.* **52** (6), 2861–2867. https://doi.org/10.1167/iovs.10-5960 (2011).
5. Huneau, C., Benali, H. & Chabriat, H. Investigating human neurovascular coupling using functional neuroimaging: A critical review of dynamic models. *Front. NeuroSci.* **9**, 467. https://doi.org/10.3389/fnins.2015.00467 (2015).
6. Baruah, J., Vasudevan, A. & Köhling, R. Vascular integrity and signaling determining brain development, network excitability, and epileptogenesis. *Front. Physiol.* **10**, 1583. https://doi.org/10.3389/fphys.2019.01583 (2020).
7. Lanigan, L. P., Clark, C. V. & Hill, D. W. Retinal circulation responses to systemic autonomic nerve stimulation. *Eye* **2** (4), 412–417. https://doi.org/10.1038/eye.1988.75 (1988).
8. Pournaras, C. J., Rungger-Brändle, E., Riva, C. E., Hardarson, S. H. & Stefansson, E. Regulation of retinal blood flow in health and disease. *Prog. Retin. Eye Res.* **27** (3), 284–330. https://doi.org/10.1016/j.preteyeres.2008.02.002 (2008).
9. Kaplan, L., Chow, B. W. & Gu, C. Neuronal regulation of the blood-brain barrier and neurovascular coupling. *Nat. Rev. Neurosci.* **21** (8), 416–432. https://doi.org/10.1038/s41583-020-0322-2 (2020).
10. Neumaier, F. et al. Retinal vessel responses to flicker stimulation are impaired in Cav2.3-Deficient Mice—An in-vivo evaluation using retinal vessel analysis (RVA). *Front. Neurol.* **12**, 659890. https://doi.org/10.3389/fneur.2021.659890 (2021).
11. Ye, X. D., Laties, A. M. & Stone, R. A. Peptidergic innervation of the retinal vasculature and optic nerve head. *Investig. Ophthalmol. Vis. Sci.* **31** (9), 1731–1737 (1990).
12. Kotliar, K. E., Vilser, W., Nagel, E. & Lanzl, I. M. Retinal vessel reaction in response to chromatic flickering light. *Graefe's Archive Clin. Experimental Ophthalmol.* **242** (5), 377–392. https://doi.org/10.1007/s00417-003-0847-x (2004).
13. Ehinger, B. Adrenergic nerves to the eye and to related structures in man and in the Cynomolgus monkey (Macaca Irus). *Investig. Ophthalmol. Vis. Sci.* **5** (1), 42–52 (1966).
14. Laties, A. M. Central retinal artery innervation: absence of adrenergic innervation to the intraocular branches. *Arch. Ophthalmol.* **77** (3), 405–409. https://doi.org/10.1001/archopht.1967.00980020407021 (1967).
15. Neuhuber, W. & Schrödl, F. Autonomic control of the eye and the iris. *Auton. Neurosci.* **165** (1), 67–79. https://doi.org/10.1016/j.autneu.2010.10.004 (2011).
16. Greenwood, J., Penfold, P. L. & Provis, J. M. Evidence for the intrinsic innervation of retinal vessels: anatomical substrate of autoregulation in the retina? In *Nervous Control of the Eye* (eds Burnstock, G. & Sillito, A. M.) 155–170 (Harwood Academic, 2000).
17. Kur, J., Newman, E. A. & Chan-Ling, T. Cellular and physiological mechanisms underlying blood flow regulation in the retina and choroid in health and disease. *Prog. Retin. Eye Res.* **31** (5), 377–406. https://doi.org/10.1016/j.preteyeres.2012.04.004 (2012).
18. Willie, C. K., Tzeng, Y., Fisher, J. A. & Ainslie, P. N. Integrative regulation of human brain blood flow. *J. Physiol.* **592** (5), 841–859. https://doi.org/10.1113/jphysiol.2013.268953 (2014).
19. Burns, S. A., Elsner, A. E. & Gast, T. J. Imaging the retinal vasculature. *Annual Rev. Vis. Sci.* **7** (1), 1–25. https://doi.org/10.1146/annurev-vision-093019-113719 (2021).
20. Tang, X., Tzekov, R. & Passaglia, C. L. Retinal cross talk in the mammalian visual system. *J. Neurophysiol.* **115** (6), 3018–3029. https://doi.org/10.1152/jn.01137.2015 (2016).
21. Innocenti, G. M. Growth and reshaping of axons in the establishment of visual callosal connections. *Science* **212** (4496), 824–827. https://doi.org/10.1126/science.7221566 (1981).
22. McLoon, S. C. & Lund, R. D. Transient retinofugal pathways in the developing chick. *Exp. Brain Res.* **45** (1–2), 277–284. https://doi.org/10.1007/bf00235788 (1982).
23. Nakamura, H. & O'Leary, D. Inaccuracies in initial growth and arborization of chick retinotectal axons followed by course corrections and axon remodeling to develop topographic order. *J. Neurosci.* **9** (11), 3776–3795. https://doi.org/10.1523/jneurosci.09-11-03776.1989 (1989).
24. Honrubia, F. M. & Elliott, J. H. Efferent innervation of the retina: I. Morphologic study of the human retina. *Arch. Ophthalmol.* **80** (1), 98–103. https://doi.org/10.1001/archopht.1968.00980050100017 (1968).
25. Honrubia, F. M. & Elliott, J. H. Efferent innervation of the retina. II. Morphologic study of the monkey retina. *Invest. Ophthalmol.* **9** (12), 971–976 (1970).
26. Terubayashi, H., Fujisawa, H., Itoi, M. & Ibata, Y. Hypothalamo-retinal centrifugal projection in the dog. *Neurosci. Lett.* **40** (1), 1–6. https://doi.org/10.1016/0304-3940(83)90082-4 (1983).
27. Labandeira-Garcia, J. L., Guerra-Seijas, M. J., Gonzalez, F., Perez, R. & Acuña, C. Location of neurons projecting to the retina in mammals. *Neurosci. Res.* **8** (4), 291–302. https://doi.org/10.1016/0168-0102(90)90035-d (1990).
28. Gastinger, M. J., Tian, N., Horvath, T. & Marshak, D. W. Retinopetal axons in mammals: emphasis on Histamine and serotonin. *Curr. Eye Res.* **31** (7–8), 655–667. https://doi.org/10.1080/02713680600776119 (2006).
29. Repérant, J. et al. The centrifugal visual system of vertebrates: A comparative analysis of its functional anatomical organization. *Brain Res. Rev.* **52** (1), 1–57. https://doi.org/10.1016/j.brainresrev.2005.11.008 (2006).
30. Murcia-Belmonte, V. et al. A Retino-retinal projection guided by Unc5c emerged in species with retinal waves. *Curr. Biol.* **29** (7), 1149–1160e4. https://doi.org/10.1016/j.cub.2019.02.052 (2019).
31. Usai, C., Ratto, G. M. & Bisti, S. Two systems of branching axons in Monkey's retina. *J. Comp. Neurol.* **308** (2), 149–161. https://doi.org/10.1002/cne.903080202 (1991).
32. Schütte, M. Centrifugal innervation of the rat retina. *Vis. Neurosci.* **12** (6), 1083–1092. https://doi.org/10.1017/s0952523800006738 (1995).
33. Gastinger, M. J. et al. Abnormal centrifugal axons in streptozotocin-diabetic rat retinas. *Investig. Ophthalmol. Vis. Sci.* **42** (11), 2679–2685 (2001).
34. Miceli, D., Repérant, J., Bertrand, C. & Rio, J. P. Functional anatomy of the avian centrifugal visual system. *Behav. Brain. Res.* **98** (2), 203–210. https://doi.org/10.1016/s0166-4328(98)00085-0 (1999).
35. Jacobson, J. H. & Suzuki, T. A. Effects of optic nerve section on he ERG. *Arch. Ophthalmol.* **67** (6), 791–801. https://doi.org/10.1001/archopht.1962.00960020791015 (1962).

36. Molotchnikoff, S., Lachapelle, P. & Casanova, C. Optic nerve Blockade influences the retinal responses to flash in rabbits. *Vision. Res.* **29** (8), 957–963. https://doi.org/10.1016/0042-6989(89)90110-7 (1989).
37. Thanos, S. Genesis, neurotrophin responsiveness, and apoptosis of a pronounced direct connection between the two eyes of the chick embryo: A natural error or a meaningful developmental event?? *J. Neurosci.* **19** (10), 3900–3917. https://doi.org/10.1523/jneurosci.19-10-03900.1999 (1999).
38. Nadal-Nicolás, F. M. et al. Retino-retinal projection in juvenile and young adult rats and mice. *Exp. Eye Res.* **134**, 47–52. https://doi.org/10.1016/j.exer.2015.03.015 (2015).
39. Ortiz, G., Odom, J. V., Passaglia, C. L. & Tzekov, R. T. Efferent influences on the bioelectrical activity of the retina in primates. *Doc. Ophthalmol.* **134** (1), 57–73. https://doi.org/10.1007/s10633-016-9567-5 (2017).
40. Koch, E. et al. Morphometric analysis of small arteries in the human retina using adaptive optics imaging: relationship with blood pressure and focal vascular changes. *J. Hypertens.* **32** (4), 890–898. https://doi.org/10.1097/hjh.0000000000000095 (2014).
41. Zacharria, M., Lamory, B. & Chateau, N. New view of the eye. *Nat. Photonics.* **5** (1), 24–26. https://doi.org/10.1038/nphoton.2010.298 (2011).
42. Jordão, J. et al. Neurovascular coupling reflex - Contralateral stimulation apparatus and setup. In: 2023 IEEE 7th Portuguese meeting on bioengineering (ENBENG), pp 28–31. (2023). https://doi.org/10.1109/enbeng58165.2023.10175365
43. Sliney, D. et al. Adjustment of guidelines for exposure of the eye to optical radiation from ocular instruments: statement from a task group of the international commission on Non-Ionizing radiation protection (ICNIRP). *Appl. Opt.* **44** (11), 2162–2176. https://doi.org/10.1364/ao.44.002162 (2005).

Acknowledgements

We are grateful to Nuno Gouveia and Ana Luís Carreira for identifying patients, Hugo Quental and Sílvia Simão for all data acquisitions, Joana Domingues for handling all subjects and segmenting all images, and Sérgio Rodrigues for his collaboration in developing the segmentation tool used in this work.

Author contributions

JJ: Software, Hardware, Formal analysis, Validation, Writing – first draft & review. JF: Subjects inclusion/exclusion criteria, Methodology, Formal analysis, Validation, Writing – review. MM: Methodology, Hardware, Formal analysis, Validation, Writing – review & editing. PG: Formal analysis, Validation, Writing – review & editing. PS: Formal analysis, Validation, Writing – review & editing. DCF: Subjects inclusion/exclusion criteria, Methodology, Formal analysis, Validation, Writing – review. DCD: Methodology, Formal analysis, Validation, Writing – review & editing. MC-B: Subjects inclusion/exclusion criteria, Methodology, Formal analysis, Investigation, Validation, Writing – review & editing, Funding acquisition, Resources. MP: Subjects inclusion/exclusion criteria, Methodology, Formal analysis, Validation, Writing – review & editing. RB: Conceptualization, Project administration, Supervision, Subjects inclusion/exclusion criteria, Methodology, Software, Hardware, Formal analysis, Validation, Writing – review & editing, Funding acquisition, Resources.

Funding

This study was supported by The Portuguese Foundation for Science and Technology (FCT) through the 2022.07585.PTDC project (DOI:https://doi.org/10.54499/2022.07585.PTDC), UI/BD/154285/2022 (Ph.D. grant), FCT/UIDB/4950/Base/2020 (DOI:https://doi.org/10.54499/UIDB/04950/2020), FCT/UIDP/4950/Programatico/2020 (DOI:https://doi.org/10.54499/UIDP/04950/2020), FCT/UIDB/4950/Base/2025 and FCT/UIDP/4950/Programatico/2025.

Declarations

Competing interests

The authors declare no competing interests.

Additional information

Supplementary Information The online version contains supplementary material available at https://doi.org/10.1038/s41598-025-98631-7.

Correspondence and requests for materials should be addressed to R.B.